Organic & Biomolecular Chemistry

Cite this: *Org. Biomol. Chem.*, 2011, **9**, 4856

www.rsc.org/obc

PAPER

Towards new ligands of nuclear receptors. Discovery of malaitasterol A, an unique bis-secosterol from marine sponge *Theonella swinhoei*†

Simona De Marino,[a] Valentina Sepe,[a] Maria Valeria D'Auria,[a] Giuseppe Bifulco,[b] Barbara Renga,[c] Sylvain Petek,[d] Stefano Fiorucci[c] and Angela Zampella*[a]

Received 10th March 2011, Accepted 8th April 2011
DOI: 10.1039/c1ob05378g

Malaitasterol A, an unprecedented bis-secosterol, was isolated from a Solomon collection of *Theonella swinhoei*. The structure was elucidated on the basis of a combination of comprehensive 1D and 2D NMR analysis, high-resolution mass spectrometry and DFT ^{13}C chemical shift calculations. The biological characterization of malaitasterol A provided evidence that this compound is a potent agonist of pregnane-X-receptor and its putative binding mode to PXR has been obtained through docking calculations.

Introduction

Marine sponges have the peculiar capability of producing highly oxidized sterol metabolites arising from distinctive pathways.[1] Among the growing number of polar sterols so far described,[2] the secosteroids feature a bond cleavage in the rings of the steroid tetracyclic nucleus.[3] Even if the large majority of secosteroids isolated from marine sponges are 9,11-secosteroids, 5,6-, 9,10-, 8,9-, 8,14- and 13,17-secosteroids were also reported. Secosteroids have been found to exhibit diverse biological activities, such as antiproliferative, antifouling, anti-inflammatory, antimicrobial, ichthyotoxic and antiviral.

In our studies of bioactive compounds from sponges collected from the Solomon Islands,[4] we found a single specimen of the sponge *Theonella swinhoei* (Order Lithistida, Class Demospongia), collected on an isolated reef off the western coast of Malaita Island, as an extraordinary source of new metabolites. Analysis of the polar extracts afforded anti-inflammatory perthamides C-D,[5,6] solomonamides A-B,[7] and two sulfated sterols, solomonsterols A and B.[8]

Investigation of the apolar extracts uncovered an unprecedented secosterol, which we named malaitasterol A. Malaitasterol A (**1**) features an unique 11,12-13,14-bis-secosteroid structure, which was deduced by interpretation of spectroscopic data, whereas DFT ^{13}C calculations were used for the assignment of the C-15 configuration.

Results and discussion

Malaitasterol A (**1**, Fig. 1) was isolated as a white amorphous solid. HR-ESIMS established the molecular formula $C_{30}H_{48}O_4$, with seven degrees of unsaturation. The ^{13}C NMR spectrum of **1** (Table 1, C_6D_6), interpreted with the help of the HSQC experiment, showed the presence of 30 carbon atoms, including one ketone carbonyl (δ_C 197.4), six sp^2 carbons, four of which were unprotonated (δ_C 129.5, 147.3, 151.7, 156.7), and two were sp^2 methylenes (δ_C 104.2, δ_H 4.59 and 5.22; δ_C 114.4, δ_H 4.85 and 4.87); three oxygen-bearing methine carbons (δ_C 72.2, 72.6 and 88.7), six methyls, eight sp^3 methylenes, five sp^3 methines, and one sp^3 unprotonated carbon (δ_C 38.5).

The ^1H NMR spectrum of **1** (Table 1, C_6D_6), in addition to the four broad singlets assigned to the sp^2 methylene protons, showed two methyl singlets (δ_H 0.74 and 1.73), three methyl doublets (δ_H 0.90, 0.91 and 0.96), one methyl triplet (δ_H 0.93, t, J = 7.4 Hz), a series of multiplets between δ_H 1.00 and 2.60, and three carbinol methine resonances at δ_H 3.63, 4.71 and 5.15.

Structure determination of the AB ring system began with an HMBC correlation from Me-19 to C-1, C-5, C-9, and C-10. COSY and TOCSY correlations delineated the spin system H-1 through OH-11, which included one hydroxyl group at C-3 and an exocyclic CH_2 group at C-4 (Fig. 2). Proton signals due to H_2-7 (δ_H 2.24 and 2.39) showed chemical shifts consistent with allylic hydrogens and a double bond at the C-8/C-9 position was assigned on the basis of the diagnostic HMBC cross-peak from Me-19 to C-9 at δ_C 156.7. The homoallylic coupling between H-11 at δ_H 5.15 (δ_C 88.7) and H-7β secured the linkage of an oxygenated methine carbon at C-11, further confirmed by HMBC correlations from H-11 to C-8 and C-10 (Fig. 2).

[a]*Dipartimento di Chimica delle Sostanze Naturali, Università di Napoli "Federico II", via D. Montesano 49, 80131 Napoli, Italy. E-mail: azampell@unina.it; Fax: +39-081676552; Tel: +39-081678525*

[b]*Dipartimento di Scienze Farmaceutiche, Università di Salerno, via Ponte don Melillo, 84084 Fisciano (SA), Italy*

[c]*Dipartimento di Medicina Clinica e Sperimentale, Università di Perugia, Nuova Facoltà di Medicina e Chirurgia, Via Gerardo Dottori 1, S. Andrea delle Fratte, 06132 Perugia, Italy*

[d]*Institut de Recherche pour le Développement (IRD), Polynesian Research Center on Island Biodiversity, BP529, 98713 Papeete, Tahiti, French Polynesia*

† Electronic supplementary information (ESI) available: Spectroscopic data and DFT ^{13}C calculated values for **1**. See DOI: 10.1039/c1ob05378g

Table 1 NMR spectroscopic data (700 MHz, C_6D_6) for malaitasterol A (**1**)

Position	δ_H	δ_C	Key HMBC	Key ROESY
1α	1.40 ovl	33.6		H-3α, H-5α
1β	1.34 ovl			H-11, Me-19
2α	1.77 m	32.5		
2β	1.27 ovl		C3	H-11, Me-19
3α	3.63 dd (5.7, 11.9)	72.6		H-5α, H-1α
4	—	151.7		
5α	1.57 br d (12.7)	45.4	C4, C10, C7, C6, C19	H-3α, H-7α
6α	1.30 ovl	20.3	C5, C10, C7	
6β	1.46 ovl		C7, C10, C5, C8, C4	
7α	2.24 ddd (7.3, 12.1, 18.2)	22.7	C9, C8, C6	H-5α
7β	2.39 ddd (1.9, 6.3, 18.2)		C14, C9, C8, C5, C6	
8	—	129.5		
9	—	156.7		
10	—	38.5		
11β	5.15 br s	88.7	C8, C10, C15	Me-19, H-1β, H-2β
12	4.87 br s	114.4	C17, C18, C13	Me-19
	4.85 br s			
13	—	147.3		
14	—	197.4		
15	4.71 dd (3.9, 6.7)	72.2	C14, C16, C17	
16	2.08 ddd (3.9, 9.4, 14.2)	32.4	C13, C14, C17	
	2.35 ddd (6.7, 10.3, 14.2)		C13, C14	
17	2.63 m	48.9		
18	1.73 s	19.2	C13, C12, C17	
19	0.74 s	18.7	C1, C5, C9, C10	H-1β, H-2β, H-11, H-12
20	1.48 ovl	35.5		
21	0.96 d (6.7)	18.1		
22	1.20 ovl	32.6		
	1.64 ovl			
23	1.20 ovl	27.4		
	1.48 ovl			
24	1.04 m	46.4		
25	1.75 m	29.3	C24, C23, C28, C26	
26	0.90 d (6.9)	19.3	C25, C27, C24	
27	0.91 d (6.9)	19.7		
28	1.22 ovl	23.4		
	1.37 ovl			
29	0.93 t (7.4)	12.6	C28, C24	
30	5.22 br s	104.2	C3, C4, C5	
	4.59 br s			
OH-11	1.81 br s	—		

Coupling costants are in parentheses and given in hertz. ^{1}H and ^{13}C assignments aided by COSY, TOCSY, ROESY, HSQC and HMBC experiments. Ovl: signals overlapped.

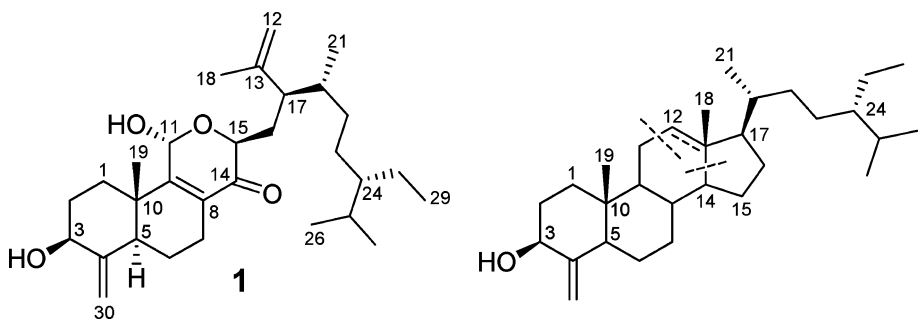

Fig. 1 Structure of malaitasterol A (**1**, left) and theonellasterol-like skeleton (right)[9] with a schematic representation of broken bonds in rings C and D of steroidal tetracyclic nucleus.

A second spin system, starting from the carbinol at δ_H 4.71 (H-15, dd, J = 3.9, 6.7 Hz) through H_2-16/H-17 linked to a C-20/C-29 steroidal 24-ethyl side chain, was easily deduced by DQF-COSY spectroscopy (Fig. 2).

The allylic coupling between the methyl singlet at δ_H 1.73 (Me-18) and the sp^2 methylene at δ_H 4.85–4.87 and the HMBC correlations Me-18 to C-13 and C-12 disclosed the 2-substituted propenyl spin system C-12/C-13/C-18.

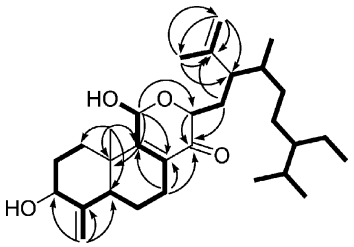

Fig. 2 COSY/TOCSY connectivities (bold bonds) and key HMBC correlations (arrows) for malaitasterol A (**1**).

The connection of the three spin systems and of the ketone carbonyl, evidenced by the ^{13}C NMR spectrum, was possible on the basis of diagnostic HMBC correlations and chemical shift considerations.

The ketone carbonyl was placed between C-8 and C-15 on the basis of the HMBC correlations H-15, H_2-16 and H-7β to the carbonyl at δ_C 197.4 and of the chemical shifts of C-9 and H-15. HMBC correlations H_2-12 and Me-18 to C-17 connected the 2-propenyl unit to C-17 (Fig. 2).

Finally, the additional degree of unsaturation required by the molecular formula of **1** was satisfied by a hemiacetal bridge between C-11 and C-15, as evidenced by the HMBC correlation H-11 to C-15 and chemical shifts of C-11 and H-11.

Therefore, the complete planar structure for malaitasterol A (**1**) was secured as depicted in Fig. 1. The coupling constants between H-3 [3.63 (dd, J = 5.7, 11.9 Hz)] and H_2-2, and the ROESY correlations, shown in Fig. 3, of H-3 with H-5 and H-1α, indicated that H-3 was axial. The ROESY correlations of H-11 with Me-19, H-1β and H-2β implied that OH-11 was α-oriented. The configuration of C-24 was determined by comparison of ^{13}C NMR data with the epimeric steroidal side chain,[10,11] whereas the absolute steroidal configuration was assumed on biogenetic grounds as depicted in Fig. 1.

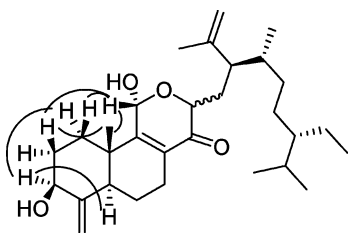

Fig. 3 ROESY correlations (arrows) for malaitasterol A (**1**).

The absence of diagnostic ROESY correlations from H-15 didn't allow us to assign the configuration of this stereocenter.

To address this issue, an NMR-QM (quantum mechanical)[12,13] method was used and two possible C-15 epimers of malaitasterol A (**1a** and **1b** in Fig. 4) were built. Subsequently, a conformational search, performed by molecular mechanics and dynamics calculations, provided the minimum energy conformer for each stereoisomer.

The two structures were optimized at the MPW1PW91 level, using the 6-31G(d) basis set. Following our previously reported protocol,[14] ^{13}C single-point calculation, using the same functional and the 6-31G(d,p) basis set, was performed on the two stereoisomers. To discriminate between the two stereoisomers, the calculated ^{13}C chemicals shifts were compared with the experimental data of **1**. In particular, concerning ^{13}C chemical shifts, preliminary considerations based on $\Delta\delta = \delta_{exp} - \delta_{calcd.}$ and MAE parameters (Mean Absolute Error, Table S1 in the ESI†) pointed to stereoisomer **1b**, displaying a MAE of 1.65 *versus* 3.00 for **1a**. Moreover, a careful analysis was done on individually calculated ^{13}C chemical shifts of nuclei around ring C (C-15, C-16, C-17, and C-18; Table S1† and Fig. 4), which were expected to experience larger variations upon inversion of configuration at C-15, finally suggesting the exclusion of stereoisomer **1a**.

In conclusion, the application of the QM method allowed us to assigned the absolute configuration at C-15 as *S*. Further confirmation derived from a retrospective analysis of the ROESY spectrum showing an intense cross-peak H-12 (4.87)/Me-19, compatible exclusively with the stereoisomer **1b**.[15]

Malaitasterol A shares some structural features with sterols so far isolated from Theonella sponges,[9,16–20] such as the 4-methylene group and the 24-alkylation, that appear distinctive of steroids from Theonella genus. Two 8,14-secosteroids, swinhosterols A and B, have been isolated from an Hokinawa collection of *Theonella swinhoei*.[21] However, the bis-secosteroid structure of **1** appears without precedent from natural sources.

Biological activity

As a part of our continuing research directed toward the discovery of marine natural nuclear receptor (NRs) ligands,[22] we have recently reported the isolation of solomonsterols A and B,[8] potent PXR agonists and new pharmacological anti-inflammatory leads, from the polar extracts of this sponge. Following this consideration, we decided to investigate whether malaitasterol A (**1**) might act as a modulator of two well characterized nuclear receptors, the farnesoid-X-receptor (FXR) and pregnane-X-receptor (PXR), highly expressed in the mammalian liver. For this purpose **1** was challenged in a reporter gene assay using an human hepatocyte cell line (HepG2 cells). While malaitasterol A (**1**), at a concentration of 10 μM, failed to activate FXR or to antagonize FXR transactivation induced by CDCA (Fig. 5A), it was a potent inducer of PXR transactivation boosting the receptor activity by 4–5 fold (Fig. 5B, $n = 4$; $P < 0.05$ *versus* untreated) and

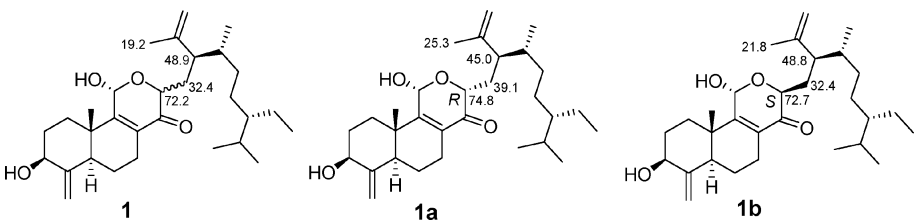

Fig. 4 C-15 epimers (**1a**, **1b**) of malaitasterol A (**1**) and comparison between experimental and calculated ^{13}C chemical shifts of nuclei around C-15.

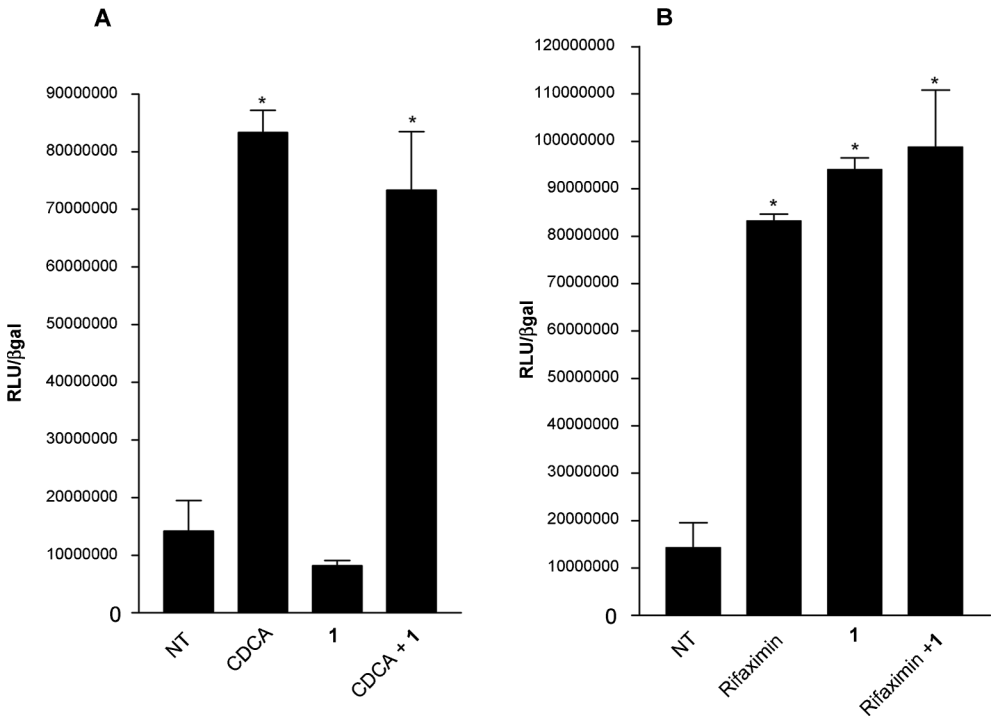

Fig. 5 (**A**) Luciferase reporter assay performed on HepG2 transiently transfected with pSG5FXR, pSG5RXR, pCMV-bgal, p(hsp27)TKLUC vectors and stimulated 18 h with CDCA, 10 μM, and **1**, 10 μM; or CDCA, 10 μM, in combination with **1**, 50 μM ($n = 4$); (**B**) Luciferase reporter assay performed on HepG2 transiently transfected with pSG5PXR, pSG5RXR, pCMV-bgal, p(cyp3a4)TKLUC vectors and stimulated 18 h with rifaximin, 10 μM, and **1**, 10 μM; or rifaximin, 10 μM, in combination with **1**, 50 μM. * $P < 0.05$ *versus* not treated (NT).

was at least as potent as rifaximin, a well characterized ligand for the human PXR.[23]

To give support to the potential PXR agonist activity of **1**, we have then tested its effects on the expression of genes that are regulated in a PXR dependent manner. Effectively malaitasterol A (**1**) stimulated the expression of three PXR target genes, CYP3A4, MDR1 and SULT2A1, in the same cell line (Fig. 6; $n = 4$; $P < 0.05$).

Docking results

We have then analyzed, by means of molecular docking calculations, the interactions of malaitasterol A (**1**) with human PXR (hPXR), in order to obtain information on its binding mode at the atomic level. All the calculations were run by Autodock4.2 software.[24]

The hPXR binding cavity volume of 1150 Å is substantially larger than that of many other nuclear receptors, including the progesterone, estrogens, retinoid and thyroid hormone receptors. Therefore hPXR is able to bind both small and large ligands. As already reported,[25–28] this region is formed by hydrophobic (Phe251, Phe288, Phe429, Cys284, Leu206, Leu209, Leu324, Leu411, Met243, Met425, Trp299), polar and charged (Ser247, Ser208, His407, Asp205, Arg410, Gln285) amino acids. In our previous work,[8] we reported the possible interactions of solomonsterols A and B with hPXR. In this model, the 2-*O* and 3-*O* sulfate groups exert hydrogen bonds with His407 and Ser247, respectively. For small molecules, such as SR 12813,[26] the possibility of having three distinct binding modes in the ligand-binding cavity of hPXR has been shown. These orientations were identified during structural refinement and were confirmed by crystallographic data.[26]

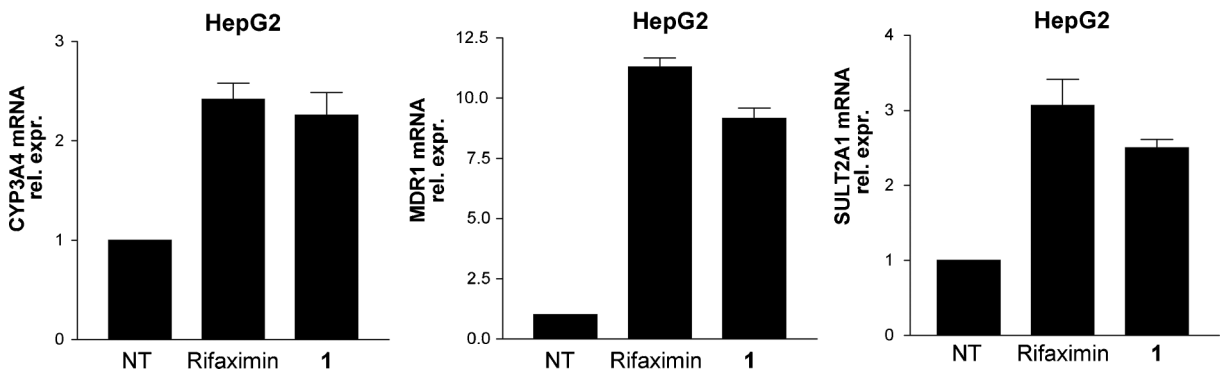

Fig. 6 Quantitative RT-PCR carried out on HepG2 cells treated with 10 μM of rifaximin or **1**.

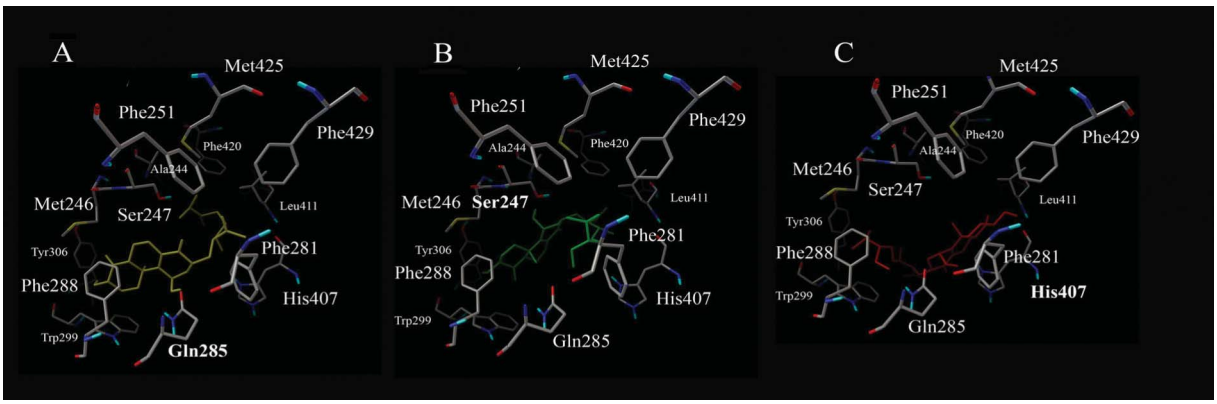

Fig. 7 Three dimensional models of the docking pose of **1** with hPXR: pose A (yellow), pose B (green) and pose C (red).

As shown in Fig. 7, for malaitasterol A (**1**) it is also possible to single out three different docking poses. Each orientation forms distinct interactions with residues that line the ligand-binding cavity of PXR. Pose A (Fig. 7**A**) shows the lowest binding energy (highest in absolute value) and consequently the most significant inhibition constant (K_I). The other two poses are different for a binding energy less than 1.0 kcal mol^{-1} with respect to pose A (see Table S2 in the ESI†). In pose A (Fig. 7**A**), **1** displays van der Waals contacts with the side chains of twelve amino acid residues. In particular, malaitasterol A side chain interacts with Leu411, Phe281, Phe420 and Ala244. Moreover the OH group at position-11 forms two hydrogen bonds with Gln285, one with NH_2 (2.12 Å) and one with the CO (1.8 Å) group of the side chain of this residue. In the pose B (Fig. 7**B**), rings A and B of malaitasterol A (**1**) display van der Waals contacts with Trp299, Phe288, Tyr306 and Met246. Once again the OH group at position-11 forms a hydrogen bond interaction (2.0 Å), but in this case with a Ser247. It is noteworthy that, in this second pose, the side chain of malaitasterol A displays the same hydrophobic contacts as pose A. In the third pose (pose C, Fig. 7**C**), **1** displays van der Waals contacts with fifteen amino acid residues of the ligand-binding cavity and the OH group at position-3 forms one hydrogen bond with His407 (1.8 Å). This pose shows, however, the weaker inhibition constant of complex (see Table S2 in the ESI†).

Conclusion

In the present report, we describe the isolation, structural characterization and pharmacological profile of an unprecedented molecule from a South Pacific specimen of the widely studied sponge *T. swinhoei*. Malaitasterol A (**1**) represents the first example of a 11,12-13,14-bis-secosterol from marine organisms.

The pharmacological screening demonstrated that, while malaitasterol A does not activate the farnesoid-X-receptor, this agent is effectively a ligand for PXR. PXR is a master gene orchestrating the expression of a wide family of genes involved in uptake, metabolism and disposal of a number of endo- and xeno-biotics, including drugs, bile acids, steroid hormones and metabolic intermediates in mammalian cells.[29] Following ligand binding, PXR forms an heterodimer with the retinoid-X-receptor (RXR) that binds to specific PXR response elements (PXREs), located in the 5′-flanking regions of PXR target genes, resulting in their transcriptional activation.[23,30,31] Supporting a role for malaitasterol A in regulating PXR, we observed that **1** effectively increased the expression of three well characterized PXR target genes in a human hepatocyte cell line.[32] Because these genes are well recognized PXR targets, these data strongly support the notion that malaitasterol A activates this receptor. These data also highlight the potential therapeutic role for this agent in regulating liver and intestinal detoxification in clinically relevant settings.

In conclusion, malaitasterol A (**1**) could be potentially used for the treatment of human disorders characterized by dysregulation of innate immunity and with inflammation, and, in light of our molecular modelling results, it can inspire the synthesis of new compounds able to target PXR. Moreover the reported putative binding mode of malaitasterol A provides insight into the mechanism of ligand recognition by PXR and paves the way to design new selective and potent modulators for human nuclear receptors.

Experimental section

General experimental procedures

Specific rotations were measured on a Perkin–Elmer 243 B polarimeter. High-resolution ESI-MS spectra were performed with a Micromass QTOF Micromass spectrometer. NMR spectra were obtained on Varian Inova 700 NMR spectrometers (^{1}H at 700 MHz, ^{13}C at 175 MHz) equipped with Sun hardware, δ (ppm), J in Hz, spectra referred to C_6HD_5 as internal standard (δ_H 7.16, δ_C 128.4). Through-space ^{1}H connectivities were evidenced using a ROESY experiment with mixing times of 200 and 500 ms, respectively. Silica gel (200–400 mesh) from Macherey-Nagel Company was used for flash chromatography. HPLC was performed using a Waters Model 510 pump equipped with a Waters Rheodine injector and a differential refractometer, model 401.

The purity of compounds was determined to be greater than 95% by HPLC, MS and NMR.

Sponge material and separation of malaitasterol A

Theonella swinhoei (order Lithistida, family Theonellidae) was collected at a depth of 22 m, on an isolated reef off the western coast of Malaita Island, Solomon Islands, in July 2004 and reference specimens are on file (R3170) at the ORSTOM, Centre

of Noumea. The samples were frozen immediately after collection and lyophilized to yield 207 g of dry mass. Taxonomic identification was performed by Dr John Hooper at Queensland Museum, Brisbane, Australia, where a voucher specimen is deposited under the accessing number G322662.

The lyophilized material (207 g) was extracted with methanol (3×2.7 L) at room temperature and the crude methanolic extract was subjected to a modified Kupchan's partitioning procedure as follows. The methanol extract was dissolved in a mixture of MeOH/H_2O containing 10% H_2O and partitioned against n-hexane (4.5 g). The water content (% v/v) of the MeOH extract was adjusted to 30% and partitioned against $CHCl_3$ (12 g). The aqueous phase was concentrated to remove MeOH and then extracted with n-BuOH (4 g).

The hexane extract was chromatographed by silica gel MPLC using a solvent gradient system from CH_2Cl_2 to CH_2Cl_2 : MeOH 1 : 1.

Fractions eluted with CH_2Cl_2 : MeOH 97 : 3 (83 mg) were further purified by HPLC on a Nucleodur 100-5 C18 (5 µm; 10 mm i.d. × 250 mm) with MeOH : H_2O (92 : 8) as eluent (flow rate 5 mL min^{-1}) to give 1.9 mg of malaitasterol A (**1**) (t_R = 13.5 min).

Malaitasterol A (**1**): white amorphous solid; $[\alpha]_D^{25}$ +0.3 (*c* 0.19, methanol); ^1H and ^{13}C NMR data in C_6D_6 given in Table 1; ESI-MS: *m/z* 479.4 $[M + Li]^+$. HRMS (ESI): calcd. for $C_{30}H_{48}LiO_4$: 479.3713; found 479.3730 $[M + Li]^+$.

Transactivation of FXR and PXR

All transfections were made using Fugene HD transfection reagent (Roche). For FXR mediated transactivation, HepG2 cells, plated in a 6-well plate at 5×10^5 cells/well, were transfected with 100 ng pSG5-FXR, 100 ng pSG5-RXR, 200 ng pCMV-galactosidase and with 500 ng of the reporter vector p(hsp27)-TK-LUC containing the FXR response element IR1 cloned from the promoter of heat shock protein 27 (hsp27). At 48 h post-transfection, cells were stimulated 18 h with 10 µM CDCA or with **1** (10 µM) alone or in combination (50 µM) with CDCA. For PXR-mediated transactivation, HepG2 cells, plated in a 6-well plate at 5×10^5 cells/well, were transfected with 100 ng pSG5-PXR, 100 ng pSG5-RXR, 200 ng pCMV-galactosidase and with 500 ng of the reporter vector containing the PXR target gene promoter (CYP3A4 gene promoter) cloned upstream of the luciferase gene (pCYP3A4promoter-TKLuc). At 48 h post-transfection, cells were stimulated 18 h with 10 µM rifaximin or **1** (10 µM) alone or in combination (50 µM) with rifaximin. Cells were lysed in 100 µL diluted reporter lysis buffer (Promega) and 20 µL of cellular lysates were assayed for luciferase activity using the Luciferase Assay System (Promega). Luminescence was measured using an automated luminometer. Luciferase activities were normalized for transfection efficiencies by dividing the relative light units by β-galactosidase activity expressed from cells cotransfected with pCMV-βgal.

Quantitative real-time PCR

50 ng template were added to the PCR mixture (final volume 25 µL) containing the following reagents: 0.2 µM of each primer and 12.5 µL of 2X SYBR Green qPCR master mix (Invitrogen, Milan, Italy). All reactions were performed in triplicate and the thermal cycling conditions were: 2 min at 95 °C, followed by 40 cycles of 95 °C for 20 s, 55 °C for 20 s and 72 °C for 30 s in an iCycler iQ instrument (Biorad, Hercules, CA). The mean value of the replicates for each sample was calculated and expressed as cycle threshold (C_T: cycle number at which each PCR reaction reaches a predetermined fluorescence threshold, set within the linear range of all reactions). The amount of gene expression was then calculated as the difference (ΔC_T) between the C_T value of the sample for the target gene and the mean C_T value of that sample for the endogenous control (GAPDH). Relative expression was calculated as the difference ($\Delta\Delta C_T$) between the ΔC_T values of the test sample and of the control sample (not treated) for each target gene. The relative quantitation value was expressed and shown as $2^{-\Delta\Delta C}{}_T$. All PCR primers were designed with PRIMER3-OUTPUT software using published sequence data from the NCBI database. The primer sequences were as follows: hGAPDH: gaaggtgaaggtcggagt and catgggtggaatcatattggaa; hSULT2A1: gatccaatctgtgcccatct and taaatcaccttggccttgga; hMDR1: gtggggcaagtcagttcatt and tcttcacctccaggctcagt; hCYP3A4: caagaccccttttgtggaaaa and cgaggcgactttctttcatc.

Computational details

The geometries of the minimum energy conformers for stereoisomers **1a** and **1b** were optimised at the hybrid DFT MPW1PW91 level of theory, using the 6-31G(d) basis set (Gaussian 09 software package).[33] GIAO ^{13}C NMR chemical shifts were performed using the MPW1PW91 functional, the 6-31G(d,p) basis set, using as input the geometry previously optimised at MPW1PW91/6-31G(d) level of theory. Molecular dynamics (MD) calculations were performed using MacroModel 8.5[34] and the MMFFs force fields at 600 K, simulation time of 5 ns and mimicking the benzene solvent using a dielectric constant of 2.27. All the sampled structures ($n = 100$) were optimised using the Polak-Ribier Coniugated Gradient algorithm (PRCG, 1000 steps, maximum derivative less than 0.05 kcal mol^{-1}).

Molecular docking calculations were performed by Autodock4.2 software[24] on quad-core Intel® Xeon® 3.4 GHz. A grid box size of $90 \times 106 \times 92$ for PXR receptor (pdb code: 1M13) with spacing of 0.375 Å between the grid points, and centered for PXR at 14.282 (*x*), 74.983 (*y*) and 0.974 (*z*) covering the active site on the two targets surface was used. The Lamarckian genetic algorithm with an initial population of 600 randomly placed individuals, a maximum number of 5.0×10^6 energy evaluations, and a maximum number of 6.0×10^6 generations were taken into account for dockings by Autodock4.2 software. A mutation rate of 0.02 and a crossover rate of 0.8 were used. Results differing by less than 3.5 Å in positional root-mean-square deviation (RMSD) were clustered together and represented by the result with the most favorable free energy of binding.

References

1 N. S. Sarma, M. S. R. Krishna and R. S. Rao, *Mar. Drugs*, 2005, **3**, 84.
2 M. V. D'Auria, L. Minale and R. Riccio, *Chem. Rev.*, 1993, **93**, 1839.
3 (*a*) D. Sica and D. Musumeci, *Steroids*, 2004, **69**, 743; (*b*) M. V. D'Auria, L. Gomez-Paloma, L. Minale, R. Riccio and C. Debitus, *Tetrahedron Lett.*, 1991, **32**, 2149.
4 Coral Reef Initiative in The South Pacific CRISP.

5 C. Festa, S. De Marino, V. Sepe, M. C. Monti, P. Luciano, M. V. D'Auria, C. Debitus, M. Bucci, V. Vellecco and A. Zampella, *Tetrahedron*, 2009, **65**, 10424.
6 V. Sepe, M. V. D'Auria, G. Bifulco, R. Ummarino and A. Zampella, *Tetrahedron*, 2010, **66**, 7520.
7 C. Festa, S. De Marino, V. Sepe, M. V. D'Auria, G. Bifulco, C. Debitus, M. Bucci, V. Vellecco and A. Zampella, *Org. Lett.*, 2011, **13**, 1532.
8 C. Festa, S. De Marino, M. V. D'Auria, G. Bifulco, B. Renga, S. Fiorucci, S. Petek and A. Zampella, *J. Med. Chem.*, 2011, **54**, 401.
9 E. Kho, D. K. Imagawa, M. Rohmer, Y. Kashman and C. Djerassi, *J. Org. Chem.*, 1981, **46**, 1836.
10 J. L. C. Wright, A. G. Mclnnes, S. Shimizu, D. G. Smith, J. A. Walter, D. Idler and W. Khalil, *Can. J. Chem.*, 1978, **56**, 1898.
11 I. Horibe, H. Nakai, T. Sato, S. Seo, K. Takeda and S. Takatsuto, *J. Chem. Soc., Perkin Trans. 1*, 1989, 1957.
12 G. Bifulco, P. Dambruoso, L. Gomez-Paloma and R. Riccio, *Chem. Rev.*, 2007, **107**, 3744.
13 S. Di Micco, M. G. Chini, R. Riccio and G. Bifulco, *Eur. J. Org. Chem.*, 2010, 1411.
14 P. Cimino, D. Duca, L. Gomez-Paloma, R. Riccio and G. Bifulco, *Magn. Reson. Chem.*, 2004, **42**, S26.
15 Measured distances H-12/Me-19: 6.6 Å in stereoisomer **1a** and 3.2 Å in stereoisomer **1b**.
16 M. Kobayashi, K. Kawazoe, T. Katori and I. Kitagawa, *Chem. Pharm. Bull.*, 1992, **40**, 1773.
17 Y. Sugo, Y. Inouye and N. Nakayama, *Steroids*, 1995, **60**, 738.
18 A. Qureshi and D. J. Faulkner, *J. Nat. Prod.*, 2000, **63**, 841.
19 R. F. Angawi, B. Calcinai, C. Cerrano, H. A. Dien, E. Fattorusso, F. Scala and O. Taglialatela-Scafati, *J. Nat. Prod.*, 2009, **72**, 2195.
20 H.-J. Zhang, Y.-H. Yi and H.-W. Lin, *Helv. Chim. Acta*, 2010, **93**, 1120.
21 A. Umeyama, N. Shoji, M. Enoki and S. Arihara, *J. Nat. Prod.*, 1997, **60**, 296.
22 V. Sepe, G. Bifulco, B. Renga, C. D'Amore, S. Fiorucci and A. Zampella, *J. Med. Chem.*, 2011, **54**, 1314.
23 X. Ma, Y. M. Shah, G. L. Guo, T. Wang, K. W. Krausz, J. R. Idle and F. J. Gonzalez, *J. Pharmacol. Exp. Ther.*, 2007, **322**, 391.
24 G. M. Morris, R. Huey, W. Lindstrom, M. F. Sanner, R. K. Belew, D. S. Goodsell and A. J. Olson, *J. Comput. Chem.*, 2009, **30**, 2785.
25 S. Ekins, C. Chang, S. Mani, M. D. Krasowski, E. J. Reschly, M. Iyer, V. A. N. Kholodovych, W. J. Welsh, M. Sinz, P. W. Swaan, R. Patel and K. Bachmann, *Mol. Pharmacol.*, 2007, **72**, 592.
26 R. E. Watkins, G. B. Wisely, L. B. Moore, J. L. Collins, M. H. Lambert, S. P. Williams, T. M. Willson, S. A. Kliewer and M. R. Redinbo, *Science*, 2001, **292**, 2329.
27 S. Ekins, S. Kortagere, M. Iyer, E. J. Reschly, M. A. Lill, M. R. Redinbo and M. D. Krasowski, *PLoS Comput. Biol.*, 2009, **5**, e1000594.
28 Y. Xue, L. B. Moore, J. Orans, L. Peng, S. Bencharit, S. A. Kliewer and M. R. Redinbo, *Mol. Endocrinol.*, 2007, **21**, 1028.
29 K. L. Rock, E. Latz, F. Ontiveros and H. Kono, *Annu. Rev. Immunol.*, 2010, **28**, 321.
30 S. Fiorucci, S. Cipriani, F. Baldelli and A. Mencarelli, *Prog. Lipid Res.*, 2010, **49**, 171.
31 A. Mencarelli, M. Migliorati, M. Barbanti, S. Cipriani, G. Palladino, E. Distrutti, B. Renga and S. Fiorucci, *Biochem. Pharmacol.*, 2010, **80**, 1700.
32 Y. M. Shah, X. Ma, K. Morimura, I. Kim and F. J. Gonzalez, *Am. J. Phys.*, 2007, **292**, G1114.
33 M. J. Frisch, G. W. Trucks, H. B. Schlegel, G. E. Scuseria, M. A. Robb, J. R. Cheeseman, G. Scalmani, V. Barone, B. Mennucci, G. A. Petersson, H. Nakatsuji, M. Caricato, X. Li, H. P. Hratchian, A. F. Izmaylov, J. Bloino, G. Zheng, J. L. Sonnenberg, M. Hada, M. Ehara, K. Toyota, R. Fukuda, J. Hasegawa, M. Ishida, T. Nakajima, Y. Honda, O. Kitao, H. Nakai, T. Vreven, J. A. Montgomery, Jr., J. E. Peralta, F. Ogliaro, M. Bearpark, J. J. Heyd, E. Brothers, K. N. Kudin, V. N. Staroverov, R. Kobayashi, J. Normand, K. Raghavachari, A. Rendell, J. C. Burant, S. S. Iyengar, J. Tomasi, M. Cossi, N. Rega, J. M. Millam, M. Klene, J. E. Knox, J. B. Cross, V. Bakken, C. Adamo, J. Jaramillo, R. Gomperts, R. E. Stratmann, O. Yazyev, A. J. Austin, R. Cammi, C. Pomelli, J. Ochterski, R. L. Martin, K. Morokuma, V. G. Zakrzewski, G. A. Voth, P. Salvador, J. J. Dannenberg, S. Dapprich, A. D. Daniels, O. Farkas, J. B. Foresman, J. V. Ortiz, J. Cioslowski and D. J. Fox, *GAUSSIAN 09 (Revision A.2)*, Gaussian, Inc., Wallingford, CT, 2009.
34 *MacroModel*, version 8.5, Schrödinger LLC, New York, NY, 2003.

